SIAM J. APPL. MATH.
Vol. 69, No. 2, pp. 348–374

STATIONARY SOLUTIONS OF DRIVEN FOURTH- AND SIXTH-ORDER CAHN–HILLIARD-TYPE EQUATIONS*

M. D. KORZEC†, P. L. EVANS‡, A. MÜNCH§, AND B. WAGNER¶

Abstract. New types of stationary solutions of a one-dimensional driven sixth-order Cahn–Hilliard-type equation that arises as a model for epitaxially growing nanostructures, such as quantum dots, are derived by an extension of the method of matched asymptotic expansions that retains exponentially small terms. This method yields analytical expressions for far-field behavior as well as the widths of the humps of these spatially nonmonotone solutions in the limit of small driving force strength, which is the deposition rate in case of epitaxial growth. These solutions extend the family of the monotone kink and antikink solutions. The hump spacing is related to solutions of the Lambert W function. Using phase-space analysis for the corresponding fifth-order dynamical system, we use a numerical technique that enables the efficient and accurate tracking of the solution branches, where the asymptotic solutions are used as initial input. Additionally, our approach is first demonstrated for the related but simpler driven fourth-order Cahn–Hilliard equation, also known as the convective Cahn–Hilliard equation.

Key words. convective Cahn–Hilliard, quantum dots, exponential asymptotics, matching, dynamical systems

AMS subject classifications. 34E05, 74K35, 65P99

DOI. 10.1137/070710949

1. Introduction.

A paradigm for phase separating systems such as binary alloys is the Cahn–Hilliard equation for the phase fraction u,

$$u_t + \left(Q(u) + \varepsilon^2 u_{xx}\right)_{xx} = 0, \tag{1.1}$$

where $Q(u)$ is the negative derivative of the double-well potential $-\mathcal{F}$, typically

$$Q(u) = \mathcal{F}'(u) = u - u^3. \tag{1.2}$$

The long-time dynamics are characterized by the logarithmically slow coarsening process of phases, corresponding to local minima of the potential, separated by interfaces of width ε. This process is described well by the motion of equidistantly spaced smoothed shock solutions or *kinks* ("positive kinks") and *antikinks* ("negative kinks") which connect the local minimum of $\mathcal{F}(u)$ at $u = -1$ to that at $u = 1$ and vice versa.

In recent years, an extension of this model has been studied for the case when the phase separating system is driven by an external field [16, 27]. In one space dimension it can be written as

$$u_t - \nu u u_x + \left(Q(u) + \varepsilon^2 u_{xx}\right)_{xx} = 0, \tag{1.3}$$

*Received by the editors December 14, 2007; accepted for publication (in revised form) June 10, 2008; published electronically November 5, 2008. This work was performed as part of Project C-10 of the DFG research center MATHEON.

http://www.siam.org/journals/siap/69-2/71094.html

†Corresponding author. Weierstrass Institute for Applied Analysis and Stochastics (WIAS), D-10117 Berlin, Germany (korzec@wias-berlin.de).

‡Institute for Mathematics, Humboldt University of Berlin, D-10099 Berlin, Germany (pevans@mathematik.hu-berlin.de).

§School of Mathematical Sciences, University of Nottingham, Nottingham NG7 2RD, UK (andreas.muench@nottingham.ac.uk). The work of this author was partially supported by the Heisenberg Fellowship of the DFG (grant MU 1626/3).

¶Weierstrass Institute for Applied Analysis and Stochastics (WIAS), D-10117 Berlin, Germany (wagnerb@wias-berlin.de).

where ν denotes the strength of the external field. This equation, the convective Cahn–Hilliard (CCH) equation, also arises as a model for the evolution of the morphology of steps on crystal surfaces [21], and the growth of thermodynamically unstable crystal surfaces into a melt with kinetic undercooling and strongly anisotropic surface tension [17, 11, 9].

The dynamics of this model as $\nu \to 0$ are characterized by coarsening, as is typical for the Cahn–Hilliard equation ($\nu = 0$) [7, 26]. If $\nu \to \infty$, using the transformation $u \mapsto u/\nu$ in (1.3) one obtains the Kuramoto–Sivashinski equation, which is a well-known model for spatiotemporal chaotic dynamics (see, e.g., [10] and references therein). Recently, Eden and Kalantarov [6] also established the existence of a finite-dimensional inertial manifold for the CCH equation, viewed as an infinite-dimensional dynamical system.

A related higher order evolution equation arises in the context of epitaxially growing thin films (for a review on self-ordered nanostructures on crystal surfaces see Shchukin and Bimberg [24]). Here, the formation of *quantum dots* and their faceting has been described by the sixth-order equation

$$u_t - \nu u u_x - \left(Q(u) + \varepsilon^2 u_{xx}\right)_{xxxx} = 0, \tag{1.4}$$

where u denotes the surface slope, ν is proportional to the deposition rate [22], and $Q(u)$ is given with (1.2); it is assumed to have this form from now on throughout the paper. The high order derivatives are a result of the additional regularization energy which is required to form an edge between two plane surfaces with different orientations. This implies that the crystal surface tension also depends on curvature, which becomes very high at edges as the parameter ε goes to zero. In analogy to the Cahn–Hilliard equation, here the phases are the orientations of the facets. This *higher order convective* Cahn–Hilliard (HCCH) equation shares many properties with the CCH equation. In both cases the dynamics are described by conserved order parameters if $\nu = 0$. They also share characteristic coarsening dynamics as $\nu \to 0$ and chaotic dynamics as ν becomes large. To understand the complicated structure of the solutions it is instructive to study first the stationary solutions and their stability, as has been done for the CCH equation [28, 16]. For small ν, the stationary solutions for both equations have been characterized by the monotone *kink* and *antikink* solutions [16, 22]. Recently new spatially nonmonotone solutions were found for the lower order equation [28]. In this study we establish that the HCCH equation also possesses such nonmonotone solutions. We show this by using phase-space methods for the corresponding fifth-order boundary value problem. We use the expression "simple" or "monotone" for a solution that connects the maximal value of $u(x)$ to the minimal value without any humps on the way down, although these extrema exist and lead to nonmonotonicity even for simple (anti-)kink solutions of the HCCH equation.

Since the treatment of this high order problem is not straightforward, one part of this study is concerned with the development of an approach that accurately locates the heteroclinic connections in the five-dimensional phase space. We find that these stationary solutions develop oscillations whose width and amplitude increase as $\nu \to 0$.

In the second part of this study we derive an analytic expression for the width and amplitude within the asymptotic regime of small external field strength. For the CCH equation we find that the width has a logarithmic dependency on the strength of the external field, while for the HCCH equation our analysis yields a dependency in terms of the Lambert W function. In order to arrive at these expressions we solve the fifth-order equation by a combination of the method of matched asymptotic expansions

and exponential asymptotics. We first demonstrate our approach for the third-order boundary value problem arising from the CCH equation. Our approach generalizes the work by Lange [15] to higher order singularly perturbed nonlinear boundary value problems, where standard application of matched asymptotics is not able to locate the position of interior layers that delimit the oscillations of the nonmonotone solutions.

Reyna and Ward [19] previously developed an approach to resolve the internal layer structure of the solutions to the boundary value problem for the related Cahn–Hilliard and viscous Cahn–Hilliard equations. The approach is based on a method due to Ward [25], who uses a "near" solvability condition for the corresponding linearized problem in his asymptotic analysis, and who was inspired by an earlier variational method [13] and work by O'Malley [18] and Rosenblat and Szeto [20], who investigated the problem of spurious solutions to singular perturbation problems of second-order nonlinear boundary value problems [3]. Moreover, for the related Kuramoto–Sivashinsky equation, a multiple-scales analysis of the corresponding third-order nonlinear boundary value problem by Adams, King, and Tew [1] shows that the derivation of monotone and oscillating traveling-wave solutions involve exponentially small terms; their method is based on an analysis of the *Stokes phenomenon* of the corresponding problem in the complex plane (see Howls, Kawai, and Takei [12] for an introduction).

In what follows we begin with the phase-space analysis for the CCH equation in section 2, followed by the asymptotic treatment for $\nu \ll 1$. The asymptotic ideas used for the CCH equation are then applied to the HCCH equation in section 3. The solutions obtained there are useful to serve as initial input for the numerical investigations of the branches of nonmonotone solutions in section 4. In this part we develop our numerical approach and then use it to identify new stationary solutions of the HCCH equation; these agree with the asymptotic theory. Finally, we briefly sum up the results together with concluding remarks in section 5.

2. Stationary solutions of the CCH equation. The high order term in the CCH equation represents the regularization of the internal layers of the solutions. For most of our investigations we consider the problem in the scaling of the internal layers, or *inner* scaling, where the x-coordinate is stretched around the location $x = \bar{x}$ of a layer according to

$$x^* = \frac{x - \bar{x}}{\varepsilon}. \tag{2.1}$$

In this scaling the CCH equation becomes (after dropping the "$*$")

$$\varepsilon^2 u_t - \frac{\delta}{2}(u^2)_x + (Q(u) + u_{xx})_{xx} = 0, \tag{2.2}$$

where $\delta = \varepsilon\nu$. The stationary problem obtained by setting u_t to zero can be integrated once, requiring that the solutions approach the constants $\pm\sqrt{A}$ as $x \to \mp\infty$, where A is a constant of integration. That is, we consider the boundary value problem

$$\frac{\delta}{2}\left(u^2 - A\right) = \left(Q(u) + u_{xx}\right)_x \tag{2.3}$$

together with the far-field conditions

$$\lim_{x\to\pm\infty} u = \mp\sqrt{A} \tag{2.4}$$

and vanishing derivatives in the same spatial limit. We refer to solutions of this system as antikinks. Monotone antikinks are known analytically [16], while recently, nonmonotone connections were computed numerically by Zaks et al. [28]. We now briefly discuss the numerical approach for obtaining these solutions. Here we concentrate on the regime where $0 < \delta \ll 1$ in order to compare the results with the asymptotic solutions derived later on. For a bifurcation analysis for larger δ we refer the reader to [28].

2.1. Numerical solutions. For the numerical solutions, we will work with a rescaled version, where we set $u = \sqrt{A}c$ so that the equilibrium points do not depend on A, and for $Q(u)$ given by (1.2), (2.3) and (2.4) become

$$(1 - c^2) = -\frac{2}{\delta\sqrt{A}}(c_{xx} + c - Ac^3)_x\,, \quad \lim_{x\to\pm\infty} c = \mp 1. \tag{2.5}$$

This differential equation could be reduced to second order by the transformation $g(c) = c_x$ at the expense of making it nonautonomous. However, for this problem we find it most convenient to present a shooting method, which enables us to track solution branches in the (A, δ) parameter plane. We transform (2.5) into a first-order system $U' = F(U)$, where $F : \mathrm{R}^3 \to \mathrm{R}^3$ is the function

$$F_1(U) = U_2, \quad F_2(U) = U_3, \quad F_3(U) = (3A(U_1)^2 - 1)U_2 + \frac{\delta\sqrt{A}}{2}((U_1)^2 - 1)\,. \tag{2.6}$$

We work in a three-dimensional phase space and denote either vectors or whole trajectories therein with capital U's. We use the same notation for two different objects because it will be clear from the context what is meant. Subscripts indicate the components.

The characteristic polynomials at the equilibrium points $U^{\pm} = (\pm 1, 0, 0)^T$ are

$$\mathcal{P}^{\pm}(\lambda) = \left|\frac{dF}{dU}(U^{\pm}) - \lambda I\right| = \lambda^3 + \lambda(1 - 3A) \mp \delta\sqrt{A}. \tag{2.7}$$

The signs of the real parts of the roots determine the dimension of the stable and unstable manifolds $W^u(U^+)$, $W^s(U^-)$, $W^s(U^+)$, $W^u(U^-)$ of the equilibrium points. The latter two are two-dimensional and so the existence of a kink is generic, while this is not the case for the antikinks. The dimension of $W^u(U^+)$ and $W^s(U^-)$ is one, so that the heteroclinic connections from the positive to the negative equilibrium arise from a codimension two intersection. This means that with the two parameters A and δ, we can expect only separated solutions when the manifolds intersect, but due to the reversibility properties, which are discussed below, the codimension reduces to one and we can expect separated solutions for the free parameter A and a fixed δ, and hence one or several whole branches in the (A, δ) parameter plane. An example of a nonmonotone connection is sketched in Figure 2.1, where the trajectories wind themselves in the phase space with a solution that exhibits 15 humps.

Reversibility and computations . It is instructive to note that the solution of (2.5) is translation invariant, $c(x) \to c(x + L)$, and that (2.6) forms a reversible dynamical system; hence it is invariant with respect to the transformation $x \to -x, U \to -U$, as has also been noted by Zaks et al. [28].

Let us consider generally a k-dimensional phase space, since the following discussion will be also useful in section 4, where we analyze the HCCH equation with its higher order system. The linear transformation

$$R : \mathrm{R}^k \to \mathrm{R}^k, \quad R(U_j) = (-1)^j U_j, \quad j = 1, \ldots, k, \tag{2.8}$$

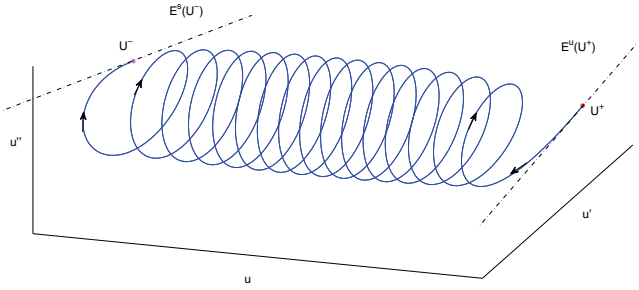

FIG. 2.1. *CCH: Antikink solutions connecting the hyperbolic equilibrium points U^+ and U^- are sought in a three-dimensional phase space. The unstable manifold emerging from U^+, $W^u(U^+)$ is one-dimensional, as is the stable manifold $W^s(U^-)$. The approximating linearized spaces $E^u(U^+)$ and $E^s(U^-)$ are drawn as dash-dotted lines and are used in the computations.*

fulfills $R^2 = Id$ and $RF(U) = -F(RU)$ for $k = 3$ and (2.6) and represents the reversibility in the phase space. It is an involution (or a reflection), and its set of fixed points is the symmetric section of the reversibility; these are zero at odd components, $U_i = 0$ for odd i. A solution that crosses such a point is necessarily symmetric under R, and for each point U on the connection there exists a corresponding transformed point RU somewhere on the branch. In fact there is an equivalence here since odd solutions necessarily cross a point in the symmetric section. It holds that c and its even derivatives have to vanish in the point of symmetry L because of the fulfilled equations $\frac{d^{2m}}{dx^{2m}}c(x+L) = -\frac{d^{2m}}{dx^{2m}}c(-x+L), m = 0, 1, \ldots, \lfloor k/2 \rfloor$, and continuity of the solution and its derivatives.

From the above we conclude that with a shooting method we can stop integrating when we find a point with zero odd components, since the second half of the solution is then given by the set of transformed points under R. Hence we define the following distance function for a trajectory U over the interval of integration which helps to find these points,

$$d_A(U) = \min_x \sqrt{\sum_{i \text{ odd}} U_i(x)^2} \, . \tag{2.9}$$

The minimization of $d_A(U)$ over the free parameter, $\min_A d_A(U)$, must result in the value zero for an antisymmetric heteroclinic solution. We can use this condition for shooting and boundary value problem formulations, for the CCH and later for the HCCH equation in section 4.

For a fixed value of δ and a range of different A we follow the relevant branch of $W^u(U^+)$ by shooting from an initial point $U^+ \pm \epsilon v$ near U^+, where v is a unit eigenvector corresponding to the positive eigenvalue of $dF/dU_{|U=U^+}$ and $\epsilon \ll 1$. We stop the integration if a certain threshold value for $|U_1|$ is crossed. Figure 2.2 shows $d_A(U)$ as a function of A for $\delta = 0.05$.

At this point we have heteroclinic connections for one fixed value of δ, which we denote by $het_k, k = 0, 1, \ldots$ (using the notation in Zaks et al. [28]). het_0 is the analytical, monotone tanh solution, while het_k has k humps on the way down from

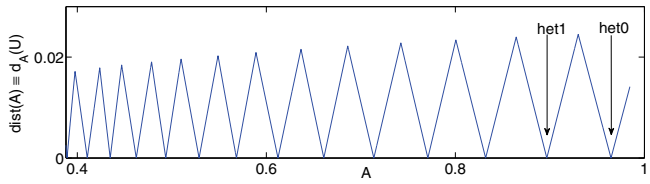

FIG. 2.2. *Distance function d_A defined by* (2.9) *depending on A with fixed $\delta = 0.05$, showing the first* 14 *zeros corresponding to het_0 to het_{13}.*

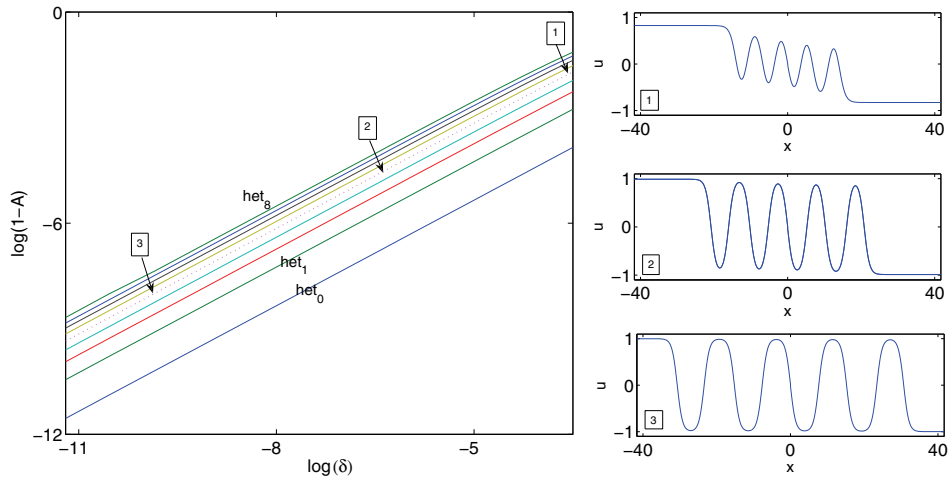

FIG. 2.3. *Parameter plane,* $\log(\delta)$ *for the x-axis and* $\log(1-A)$ *for the y-axis, for the CCH equation for the first nine antikink solutions* $het_k, k = 0, 1, \ldots, 8$. *The graphs on the right show the shapes of representative* het_4 *solutions, and hence those on the fifth line from below, for the approximate* (A, δ) *tuples* $(0.8259, 0.0289)$, $(0.9893, 0.0017)$, *and* $(0.9998, 2.6457 \cdot 10^{-5})$.

$\sqrt{A}$ to $-\sqrt{A}$. We will use the same terminology for the solution structure of the stationary HCCH problem in section 4. Here, a het_k solution corresponds to the kth zero from the right in Figure 2.2. We then follow the roots of the distance function by linearly extrapolating to a new guess for A and use a bisection algorithm to quickly converge to the next root. Figure 2.3 shows a portion of the (A, δ) parameter plane, where we concentrate on very small values of δ or, differently interpreted, on the bifurcation of the various spiraling CCH orbits from the heteroclinic connections of the Cahn–Hilliard equation in its one dimension smaller phase space.

2.2. Asymptotic internal layer analysis. For the asymptotic analysis we use a slightly different scaling than for the numerical treatment. Here, we let

$$x^* = \frac{x - \bar{x}}{\sqrt{2}\,\varepsilon} \tag{2.10}$$

denote the *inner* variable about a layer located at $x = \bar{x}$. For the stationary problem we then obtain

$$\left(u'' + 2\,Q(u)\right)' = \delta\sqrt{2}\left(u^2 - A\right) \tag{2.11}$$

instead of (2.3), where $' = d/dx^*$. For later comparisons of the numerical and asymptotic results we have to keep in mind that the spatial scales differ by a factor of $\sqrt{2}$.

We point out that the problem considered here shares the internal layer structure of the singular perturbation problems discussed by Lange [15], and we will make use of and extend this ansatz for our situation. This will also prove useful for understanding the approach taken for the HCCH problem in section 3.1, since there we have to carefully combine the exponential matching with the conventional matching procedure when matching the two regions. For both problems the asymptotic analysis can be conveniently carried out in terms of the small parameter δ.

In the following analysis we consider the simplest case of a nonmonotone solution with only one hump, as illustrated in Figure 2.4; we note that nonmonotone solutions with more oscillations can be treated similarly.

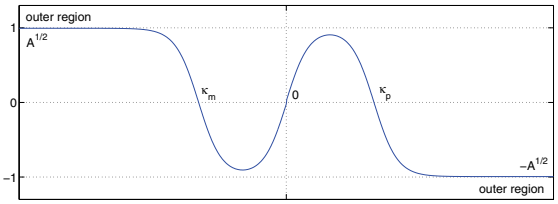

FIG. 2.4. *Sketch of a* 1*-hump, or het*$_1$*, solution showing the general setup for the matching procedure for the CCH and HCCH equations.*

2.2.1. The 1-hump solution. We observe that the 1-hump solution has three internal layers, one at $\kappa_m < 0$, one at κ_p, and one at the symmetry point in between. Since the solution is point symmetric, we can choose this point to be $x = 0$, and it will be enough to discuss only the two layers at κ_m and zero and then match them to the *outer* solution.

Internal layer near κ_m*.* For the first internal layer at κ_m we let

$$x_m = \frac{x}{\sqrt{2}\,\varepsilon} - \frac{\bar{\kappa}_m}{\sqrt{2}}, \tag{2.12}$$

where $\bar{\kappa}_m < 0$, and set

$$\kappa_m = \bar{\kappa}_m + \sqrt{2}\sum_{k=1}^{\infty} \delta^k \kappa_{mk}, \tag{2.13}$$

so that to leading order the location where the solution crosses zero is $\bar{\kappa}_m$ and the additional terms account for the corrections due to the higher order problems.

With $u_m(x_m) = u(\varepsilon(\bar{\kappa}_m + \sqrt{2}\,x_m))$ the governing equation becomes

$$u_m''' + 2\,Q'(u_m) = \delta\,\sqrt{2}\,(u_m^2 - A)\,, \quad \text{where} \quad ' = \frac{d}{dx_m}. \tag{2.14}$$

For the boundary condition where u_m crosses zero, we have

$$u_m\left(\frac{\kappa_m - \bar{\kappa}_m}{\sqrt{2}}\right) = 0, \tag{2.15}$$

and the condition towards $-\infty$ is

$$\lim_{x_m \to -\infty} u_m(x_m) = \sqrt{A}. \tag{2.16}$$

We now assume $u_m(x_m)$ can be written as the following asymptotic expansion, valid near κ_m:

$$u_\alpha(x_\alpha) = u_{\alpha 0}(x_\alpha) + \sum_{k=1}^{\infty} \delta^k \, u_{\alpha k}(x_\alpha)\,, \tag{2.17}$$

with $\alpha = m$ here. Additionally, we assume A has the asymptotic expansion

$$A = 1 + \delta A_1 + O(\delta^2). \tag{2.18}$$

Observe that from (2.16) and (2.18),

$$\lim_{x_m \to -\infty} u_m(x_m) = \lim_{x_m \to -\infty} u_{m0}(x_m) + \sum_{k=1}^{\infty} \delta^k \, u_{mk}(x_m) = 1 + \frac{1}{2} \sum_{k=1}^{\infty} \delta^k A_k\,. \tag{2.19}$$

To leading order in δ we get the following problem for the Cahn–Hilliard equation:

$$u_{m0}''' + 2\, Q'(u_{m0}) = 0, \tag{2.20a}$$

$$u_{m0}(0) = 0 \quad \text{and} \quad \lim_{x_m \to -\infty} u_{m0}(x_m) = 1 \tag{2.20b}$$

with the unique solution $u_{m0}(x_m) = -\tanh(x_m)$. Next, the problem of order δ is

$$\Big(\mathcal{L}\,(u_{m1}, x_m) \Big)' = \sqrt{2}\, \left(\tanh^2(x_m) - 1 \right), \tag{2.21a}$$

$$u_{m1}(0) = \kappa_{m1} \quad \text{and} \quad \lim_{x_m \to -\infty} u_{m1}(x_m) = \frac{A_1}{2}\,, \tag{2.21b}$$

where κ_{m1} and A_1 are constants to be exponentially matched and the operator $\mathcal{L}$ is defined by

$$\mathcal{L}(v, z) = v'' + 2 \left(1 - 3 \tanh^2(z) \right) v\,, \tag{2.22}$$

and $z = x_m$, $v = u_{m1}$, and $' = d/dx_m$. Note that the first boundary condition is obtained by expanding (2.15),

$$\begin{aligned} u_m \left(\sum_{k=1}^{\infty} \delta^k \kappa_{mk} \right) &= u_m \Big(\, \delta \kappa_{m1} + \delta^2 \kappa_{m2} + O(\delta^3) \, \Big) \\ &= u_{m0}(0) + \delta \big(\, \kappa_{m1} u'_{m0}(0) + u_{m1}(0) \big) + O(\delta^2), \end{aligned} \tag{2.23}$$

so that collecting the terms of order δ gives

$$u_{m1}(0) = -\kappa_{m1}\, u'_{m0}(0) = \kappa_{m1}\,.$$

Next, we integrate (2.21) once to obtain

$$\mathcal{L}\,(u_{m1}, x_m) = f_m(x_m)\,, \tag{2.24}$$

where $f_m(x_m) = -\sqrt{2}\tanh(x_m) + c_m$. Taking the limit of this equation to $-\infty$ yields $c_m = -\sqrt{2} - 2A_1$ so that

$$f_m(x_m) = -\sqrt{2}\,(\tanh(x_m) + 1) - 2A_1\,. \tag{2.25}$$

The homogeneous solutions of (2.24) are

$$\phi_m(x_m) = -u'_{m0}(x_m) = 1 - \tanh^2(x_m)\,, \tag{2.26}$$

$$\psi_m(x_m) = \left(\int_0^{x_m} \frac{dz}{\phi_m^2(z)}\right)\phi_m(x_m)\,. \tag{2.27}$$

Also note that $\lim_{x_m\to-\infty}\phi_m(x_m) = 0$ and $\psi_m(0) = 0$. At this stage it is convenient to choose the inhomogeneous solution that remains bounded as $x_m \to -\infty$ and vanishes at $x_m = 0$, which is satisfied by

$$\varphi_\alpha(x_\alpha) = \psi_\alpha(x_\alpha)\int_{-\infty}^{x_\alpha} \phi_\alpha\, f_\alpha\, dz - \phi_\alpha(x_\alpha)\int_0^{x_\alpha} \psi_\alpha\, f_\alpha\, dz \tag{2.28}$$

with $\alpha = m$. Hence, the unique solution for (2.21) is the linear combination

$$u_{m1}(x_m) = -\kappa_{m1}\phi_m(x_m) + \varphi_m(x_m)\,. \tag{2.29}$$

Internal layer near $x = 0$. For the internal layer near the origin we proceed as above. Here, we stretch the independent variable as

$$x_0 = \frac{x}{\sqrt{2}\varepsilon} \tag{2.30}$$

and construct an asymptotic expansion (2.17) near $x = 0$ with $\alpha = 0$ for the solution of the problem

$$u_0''' + 2\,Q'(u_0) = \delta\,\sqrt{2}\,(u_0^2 - A)\,, \quad \text{where} \quad {}' = \frac{d}{dx_0}. \tag{2.31}$$

We note that the point $x = 0$ is assumed to be the symmetry point of the complete solution; hence here we require

$$u_0(0) = 0 \quad \text{and} \quad u_0''(0) = 0\,. \tag{2.32}$$

In anticipation of the exponential matching we also require that $\lim_{x_0\to-\infty} u_{00}(x_0) = -1$, so that the solution to the leading order problem is $u_{00}(x_0) = \tanh(x_0)$. For the solution to $O(\delta)$ we find

$$u_{01}(x_0) = b_0\,\psi_0(x_0) + \varphi_0(x_0), \tag{2.33}$$

where b_0 is a further constant to be exponentially matched. Here, the homogeneous solutions are

$$\phi_0(x_0) = -u'_{00}(x_0) \quad \text{and} \quad \psi_0(x_0) = \left(\int_0^{x_0} \frac{dz}{\phi_0^2(z)}\right)\phi_0(x_0), \tag{2.34}$$

and the inhomogeneous solution is defined by (2.28), where $\alpha = 0$ and $f_0(x_0) = -\sqrt{2}\tanh(x_0)$. They are chosen such that $\varphi_0(0) = 0$ and $\varphi_0''(0) = 0$; in fact we have $\lim_{x_0\to\pm\infty}\varphi_0(x_0) = \pm\sqrt{2}/4$.

2.2.2. Exponential matching. Exponential matching requires that all exponentially small and exponentially growing terms have to be accounted for and matched. This means that first we have to express the variable x_0 in terms of x_m (or vice versa). From the definitions of these variables it follows that

$$x_0 = x_m + \frac{\bar{\kappa}_m}{\sqrt{2}}\,. \tag{2.35}$$

In particular, exponential terms in the solution $u_0(x_0)$ transform as $e^{2x_0} = e^{\sqrt{2}\bar{\kappa}_m}\, e^{2x_m}$ and so forth for higher order exponential terms e^{2nx_0} or terms with different signs in the exponent.

Now note that as $x_0 \to -\infty$, the leading and $O(\delta)$ solutions can be written as

$$u_{00}(x_0) = -1 + 2e^{2x_0} - O(e^{4x_0}), \tag{2.36}$$

and with $\bar{\mu} = \left(\frac{3}{2}b_0 + \sqrt{2}\right)$,

$$u_{01}(x_0) = -\frac{1}{4}\bar{\mu} - \frac{b_0}{16}e^{-2x_0} + \left(\frac{13}{16}b_0 + \frac{1}{\sqrt{2}} + \bar{\mu}x_0\right)e^{2x_0} + O(e^{4x_0})\,. \tag{2.37}$$

Written in x_m variables, the solution

$$\begin{aligned} u_0(x_m) &= -1 + 2e^{2x_m}e^{\sqrt{2}\bar{\kappa}_m} + O(e^{2\sqrt{2}\bar{\kappa}_m}) \\ &\quad + \delta\left(-\frac{1}{4}\bar{\mu} - \frac{b_0}{16}e^{-2x_m}e^{-\sqrt{2}\bar{\kappa}_m} + \left(\frac{13}{16}b_0 + \frac{1}{\sqrt{2}} + \bar{\mu}\left(x_m + \frac{\bar{\kappa}_m}{\sqrt{2}\varepsilon}\right)\right)e^{2x_m}e^{\sqrt{2}\bar{\kappa}_m}\right. \\ &\qquad \left. + O(e^{2\sqrt{2}\bar{\kappa}_m})\right) + O(\delta^2) \end{aligned} \tag{2.38}$$

has to be exponentially matched to

$$\begin{aligned} u_m(x_m) &= -1 + 2e^{-2x_m} + O(e^{-4x_m}) \\ &\quad + \delta\left(-\left(A_1 + \frac{\sqrt{2}}{4}\right) - \frac{1}{4}\left(A_1 + \frac{1}{\sqrt{2}}\right)e^{2x_m} + \left(\frac{7}{2}A_1 + \frac{5}{4}\sqrt{2} + 4\kappa_{m1}\right)e^{-2x_m}\right. \\ &\qquad \left. - \left(3A_1 + \frac{1}{\sqrt{2}}\right)x_m e^{-2x_m} + O\big(e^{-4x_m}\big)\right) + O(\delta^2) \end{aligned} \tag{2.39}$$

as $x_m \to \infty$. While we have already anticipated matching of the constants during the derivation of the leading order solutions, the constant terms of the $O(\delta)$ solutions are first to be matched. Matching to the exponential terms in (2.39) entails a rearranging of terms of different orders of magnitude in the expansion (2.38). In particular, the first exponential term to leading order in (2.39) matches the second term of $O(\delta)$ in (2.38), the second and largest exponential term of $O(\delta)$ in (2.39) matches the second term of the leading order in (2.38), and so forth. Summarizing, we obtain

$$\frac{1}{4}\left(\frac{3}{2}b_0 + \sqrt{2}\right) = A_1 + \frac{\sqrt{2}}{4}, \quad -\rho\frac{b_0}{16} = 2, \quad -\frac{\rho}{4}\left(A_1 + \frac{1}{\sqrt{2}}\right) = 2\,, \tag{2.40}$$

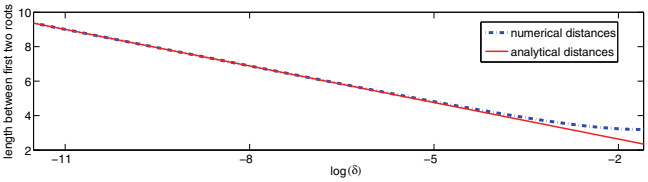

FIG. 2.5. *Distances between the first two roots of the* het_1 *solutions versus* $\log(\delta)$ *together with the width predicted by the asymptotic formula* (2.43).

where we denote $\rho = \delta\, e^{-\sqrt{2}\bar{\kappa}_m}$. Solving yields

$$\rho = 4\sqrt{2}, \quad A_1 = -\frac{3}{\sqrt{2}}, \quad \text{and} \quad b_0 = -\frac{8}{\sqrt{2}}. \tag{2.41}$$

We observe that we have determined the $O(\delta)$ correction A_1. Additionally, we now know that $\delta\, e^{-\sqrt{2}\bar{\kappa}_m} = 4\sqrt{2}$, hence

$$\bar{\kappa}_m = \frac{\ln(\delta)}{\sqrt{2}} - \frac{\ln\left(4\sqrt{2}\right)}{\sqrt{2}}, \tag{2.42}$$

and if we recall (2.13) and $\kappa_m < 0$, then the width of the hump is $-\kappa_m$, where

$$\kappa_m = \frac{\ln(\delta)}{\sqrt{2}} - \frac{\ln\left(4\sqrt{2}\right)}{\sqrt{2}} + O(\delta)\ . \tag{2.43}$$

Further constants, such as κ_{m1}, are found by including higher exponential terms and expansions of the higher order problems. Finally, we note that by making use of the symmetry of the solution about the point $x = 0$, the exponential matching of the solution near zero to the one near κ_p proceeds analogously.

2.2.3. Comparison of numerical and asymptotic solution. For the comparison with the asymptotic solution we are interested mainly in the het_1 solution which we derived in section 2.2.1. By numerical continuation of the shooting method, one obtains N tuples $(A^{(j)}, \delta^{(j)}), j = 1, \ldots, N$, in the parameter plane that give a het_1-branch when being connected. We use two vectors of parameters which we abbreviate $\mathbf{A} = (A^{(j)})_{j=1,\ldots,N}$ and $\boldsymbol{\delta} = (\delta^{(j)})_{j=1,\ldots,N}$ to confirm the formulas we obtained in the previous section. Further we make use of a distance vector $\mathbf{K} = (K^{(j)})_{j=1,\ldots,N}$. $\mathbf{K}$ contains the distances between the zero crossings of the solutions, or in context of the asymptotics section (see Figure 2.4) $K^{(j)} \approx |\kappa_m(\delta^{(j)})|$. To obtain the relation between A and δ and the evolution of the distances we solve the least squares problems

$$\min_{\mu_1} \|(\mathbf{1} - \mu_1 \boldsymbol{\delta}) - \mathbf{A}\|_2^2 \quad \text{and} \quad \min_{\eta_1,\eta_2} \|\eta_1 \log(\boldsymbol{\delta}\eta_2) - \mathbf{K}\|_2^2,$$

and hence we assume a linear law for the A-values in δ and a general logarithmic law for the distances. We obtain

$$A \approx 1 - 2.12\delta \approx 1 - \frac{3}{\sqrt{2}}\delta \quad \text{and} \quad K \approx -0.71 \log(0.18\delta), \tag{2.44}$$

which confirms the results from the analysis, (2.41) and (2.43). We see the good match in the distance plot in Figure 2.5.

These results motivated us to obtain a general rule for the relation between the two parameters of the CCH equation for different stationary solutions. The numerically computed branches in Figure 2.3 show that the slopes of the het_k branches are one when plotting $\log(\delta)$ against $\log(1-A)$, so that the relation $\log(\delta)+\text{const} = \log(1-A)$ shows the linear dependence $A(k) = 1+A_1(k)\delta$, where $A(k)$ is the A value for the het_k solution and $A_1(k)$ its linear coefficient. We see that the magnitude of A_1 increases linearly with the order k of the heteroclinic connection, and we obtain a general expression for the squared far-field value for nonmonotone het_k solutions, namely,

$$A_1(k) = -\frac{2k+1}{\sqrt{2}}\,. \tag{2.45}$$

3. Matched and exponential asymptotics for the stationary HCCH equation. As we did for the CCH equation, we will perform our analysis of the internal layers in the inner scaling (2.10). From the stationary form of (1.4) we obtain the equation

$$\left(u'' + 2\,Q(u)\right)''' = -\delta\; 2^{3/2}\left(u^2 - A\right) \tag{3.1}$$

after integrating once and requiring that for an antikink $\lim_{x\to\pm\infty} u = \mp\sqrt{A}$ and setting $\delta = \epsilon^3\nu$ here. We consider the het_1 (1-hump) solution and again make use of the point symmetry of the problem. Now, however, unlike for the CCH equation, the solutions in the *outer* region are not just constants. Here, we have to introduce an *outer* layer to the left of the *inner* layer about κ_m; see also Figure 2.4 for the case of a 1-hump solution. In the following subsections we first briefly derive the solution to this *outer* problem and match it to the solution to the *inner* problem near κ_m. The remaining degrees of freedom are then used to exponentially match it to a second inner layer near $x = 0$.

It has been demonstrated in [22] for monotone antikink solutions of the HCCH equation that it is necessary to match terms up to order δ in order to obtain the correction A_1, given the asymptotic expansion of A,

$$A = 1 + \sum_{k=1}^{\infty} \delta^{k/3}\, A_k\,. \tag{3.2}$$

Here, for the nonmonotone antikinks we have to match *inner* and *outer* solutions and then also exponentially match the *inner* layers. This has to be carried through iteratively up to three orders of magnitude in order to obtain not only the correction A_1 but also the expression for the width of the humps.

3.1. The 1-hump solution for the HCCH equation. We start by shifting to the inner coordinates that describe the region near κ_m, which is to be matched to the outer region. Again defining x_m by (2.12), the governing equation in this inner region is

$$\Big(u_m'' + 2\,Q(u_m)\Big)''' = -\,2^{3/2}\,\delta\,(u_m^2 - A), \quad \text{where} \quad {}' = \frac{d}{dx_m}. \tag{3.3}$$

For the boundary conditions we again place κ_m near the point where u_m crosses zero, i.e.,

$$u_m\left(\frac{\kappa_m - \bar{\kappa}_m}{\sqrt{2}}\right) = 0\,. \tag{3.4}$$

The condition towards $-\infty$ is not as trivial as for the CCH equation but needs to be matched to the outer solution in the region to the left of κ_m (or to the right of κ_p, taking account of symmetry).

For the *outer* region (see Figure 2.4), where x_m becomes very large, we use the ansatz

$$\xi = \delta^{1/3}\, x_m \quad \text{and} \quad Y(\xi;\delta) = u_m(x_m;\delta) \tag{3.5}$$

and obtain the *outer* problem

$$\Big(\delta^{2/3}\, Y_{\xi\xi} + 2\, Q\,(Y)\,\Big)_{\xi\xi\xi} = -\,2^{3/2}\,\left(Y^2 - A\right) \tag{3.6}$$

with the far-field condition

$$\lim_{\xi\to-\infty} Y(\xi) = \sqrt{A}\,. \tag{3.7}$$

The region near $x = 0$, for which we use the variable x_0 from (2.30), is described by the problem

$$\Big(u_0'' + 2\,Q(u_0)\Big)''' = -\,2^{3/2}\,\delta\,(u_0^2 - A) \quad \text{where} \quad {}' = \frac{d}{dx_0}. \tag{3.8}$$

The point $x = 0$ is the point of symmetry of the solution. Here we require

$$u_0(0) = 0, \quad u_0''(0) = 0, \quad \text{and} \quad u_0''''(0) = 0\,, \tag{3.9}$$

plus additional conditions from the exponential matching to the internal layer near κ_m as $x_0 \to -\infty$, as we have shown for the CCH equation.

Here we assume that the solutions to these three problems for Y, u_m, and u_0 can be represented by asymptotic expansions

$$u_\alpha(x_\alpha;\varepsilon) = u_{\alpha 0}(x_\alpha) + \sum_{k=1}^{\infty} \delta^{k/3}\, u_{\alpha k}(x_\alpha), \quad \text{where} \quad \alpha = 0, m, \tag{3.10}$$

valid near κ_m and $x = 0$, respectively, and

$$Y(\xi;\delta) = Y_0(\xi) + \sum_{k=1}^{\infty} \delta^{k/3}\, Y_k(\xi)\,, \tag{3.11}$$

valid in the outer region, where we let

$$\kappa_m = \bar{\kappa}_m + \sqrt{2}\sum_{k=1}^{\infty} \delta^{k/3} \kappa_{mk}\,. \tag{3.12}$$

Obtaining solutions to the outer problem is straightforward [22], but in order to be more comprehensible we include the results in Appendix A. The solutions to the other regions are discussed now.

3.1.1. Leading order. To leading order in δ we get the problem

$$(u''_{m0} + 2\,Q(u_{m0}))''' = 0, \tag{3.13a}$$

$$u_{m0}(0) = 0. \tag{3.13b}$$

Matching to the leading order outer solution (A.2) $Y_0 = 1$ we find

$$u_{m0}(x_m) = -\tanh(x_m)\,. \tag{3.14}$$

Its representation towards the internal layer about $x = 0$ is given by

$$u_{m0} = -1 + 2e^{-2x_m} - 2e^{-4x_m} + O(e^{-6x_m}) \tag{3.15}$$

as $x_m \to \infty$. The leading order problem for this region is

$$(u''_{00} + 2\,Q(u_{00}))''' = 0, \tag{3.16a}$$

$$u_{00}(0) = 0, \quad u''_{00}(0) = 0, \quad \text{and} \quad u''''_{00}(0) = 0, \tag{3.16b}$$

and its solution is

$$u_{00}(x_0) = \tanh(x_0)\,. \tag{3.17}$$

As $x_0 \to -\infty$, its behavior is given by

$$u_{00} = -1 + 2e^{2x_0} - 2e^{4x_0} + O(e^{6x_0})\,. \tag{3.18}$$

3.1.2. $\mathbf{O(\delta^{1/3})}$.

Internal layer near $x = \kappa_m$. The expansion of (3.3) and (3.4) to order $\delta^{1/3}$ yields

$$\mathcal{L}(u_{m1}, x_m) = f_{m1}(x_m), \tag{3.19a}$$

$$u_{m1}(0) = -u'_{m0}(0)\,\kappa_{m1} = \kappa_{m1}, \tag{3.19b}$$

where $\mathcal{L}$ is defined by (2.22) as for the CCH equation and

$$f_{m1}(x_m) := c_{1m}x_m^2 + c_{2m}x_m + c_{3m}\,. \tag{3.20}$$

The homogenous solutions are therefore (2.26) and (2.27). The constants c_{1m}, c_{2m}, c_{3m} are obtained by three successive integrations of the ODE for u_{m1} obtained at this order. We choose the inhomogeneous solution so that it grows only algebraically as $x_m \to -\infty$ and vanishes at $x_m = 0$. Particular solutions to (3.19b) are of the form

$$\varphi_{\alpha j}(x_\alpha) = \psi_\alpha(x_\alpha)\int_0^{x_\alpha} \phi_\alpha\, f_{\alpha j}\, dz - \phi_\alpha(x_\alpha)\int_0^{x_\alpha} \psi_\alpha\, f_{\alpha j}\, dz + \gamma_{\alpha j}\psi_\alpha(x_\alpha)\,, \tag{3.21}$$

so that now we obtain φ_{m1} for $\alpha = m, j = 1$ in (3.21) and

$$\gamma_{m1} = -\frac{\pi^2}{12}c_{1m} + \ln(2)c_{2m} - c_{3m}\,. \tag{3.22}$$

Hence the solution is

$$u_{m1}(x_m) = -\kappa_{m1}\phi_m(x_m) + \varphi_{m1}(x_m)\,. \tag{3.23}$$

We evaluate ψ_α, ϕ_α, etc. and subsequent functions with the assistance of *Maple*. As $x_m \to -\infty$, the limiting behavior of u_{m1} is

(3.24)
$$\begin{aligned} u_{m1}(x_m) = & -\frac{1}{8}(c_{1m}+2c_{3m}) - \frac{1}{4}c_{2m}x_m - \frac{1}{4}c_{1m}x_m^2 \\ & + \left(\frac{1}{64}(-7c_{1m}-8c_{3m}+256\kappa_{m1}+30c_{2m}+4c_{2m}\pi^2-72c_{1m}\zeta(3)) \right. \\ & \left. + \frac{1}{16}(-6c_{2m}+15c_{1m}+24c_{3m})x_m + \frac{1}{8}(6c_{2m}-3c_{1m})x_m^2 + \frac{1}{2}c_{1m}x_m^3\right) e^{2x_m} \\ & + O(\, e^{4x_m}), \end{aligned}$$

where ζ is the Riemann zeta function, and u_{m1} must match the outer solution, which is given in the appendix by (A.10) and has only constant terms to this order. Hence we require $c_{2m} = 0$ and $c_{1m} = 0$. The matched solution is now

$$\begin{aligned} u_{m1}^{(m)}(x_m) = & \left(1-\tanh^2(x_m)\right)\kappa_{m1} \\ & -\frac{c_{3m}}{16}\Big(-2e^{6x_m}+4+10e^{2x_m}-12e^{4x_m}-24x_m e^{2x_m}\Big)\frac{e^{-2x_m}}{\left(e^{2x_m}+1\right)^2}, \end{aligned} \tag{3.25}$$

where we denote by $u_{m1}^{(m)}$ the solution that is obtained by matching to the outer solution Y. As we will see later, exponential matching to the inner solution u_0, i.e., as $x_m \to \infty$, where we find

$$\begin{aligned} u_{m1}^{(m)}(x_m) = & \frac{1}{8}c_{3m}e^{2x_m} + \frac{1}{2}c_{3m} + \left(-\frac{7}{4}c_{3m}+4\kappa_{m1}+\frac{3}{2}c_{3m}x_m\right)e^{-2x_m} \\ & + \left(\frac{11}{4}c_{3m}-8\kappa_{m1}-3c_{3m}x_m\right)e^{-4x_m} + O(e^{-6x_m}), \end{aligned}$$

requires also $c_{3m} = 0$. Hence, denoting by $u_{m1}^{(e)}$ the solution that has been exponentially matched to the inner solution u_0 near $x = 0$, we obtain

$$u_{m1}^{(e)}(x_m) = \left(1-\tanh^2(x_m)\right)\,\kappa_{m1}\,. \tag{3.26}$$

Internal layer near $x = 0$. The $O(\delta^{1/3})$ problem is

$$\mathcal{L}(u_{01}, x_0) = f_{01}(x_0)\,, \tag{3.27a}$$
$$u_{01}(0) = 0, \quad u_{01}''(0) = 0, \quad \text{and} \quad u_{01}''''(0) = 0\,, \tag{3.27b}$$

with

$$f_{01}(x_0) := c_{10}x_0^2 + c_{20}x_0 + c_{30}\,. \tag{3.28}$$

Its general solution reads

$$u_{01}(x_0) = \varphi_{01}(x_0) + g_1\,\psi_0(x_0)\,, \tag{3.29}$$

where the homogeneous solutions are as before and the inhomogeneous solution is given by (3.21) with $\alpha = 0, j = 1$, and

$$\gamma_0 = -\frac{\pi^2}{12}c_{10} + \ln(2)\,c_{20} - c_{30}\,, \tag{3.30}$$

so that $\varphi_{01}(0) = 0$ and φ_{01} grows algebraically as $x_0 \to -\infty$. Furthermore, symmetry requires $\varphi''_{01}(0) = 0$ and $\varphi''''_{01}(0) = 0$, which implies $c_{10} = 0$ and $c_{30} = 0$, leading to

(3.31)
$$\begin{aligned}\varphi_{01}(x_0) = \frac{c_{20}}{16(1+e^{-2x_0})^2}\Big(&1 - 4x_0 + 12\,\mathrm{dilog}(e^{2x_0}+1)e^{-2x_0} - e^{-4x_0} + 12x_0^2 e^{-2x_0}\\ &+ \pi^2 e^{-2x_0} + 12x_0 e^{-4x_0} - 14x_0 e^{-2x_0} - \ln(1+e^{-2x_0})e^{2x_0} + 8e^{-4x_0}\ln(1+e^{-2x_0})\\ &- 8\ln(1+e^{-2x_0}) + e^{-6x_0}\ln(1+e^{-2x_0}) + 2e^{-6x_0}x_0\Big),\end{aligned}$$

where dilog denotes the dilogarithm function. The remaining free parameters of u_{01} to be matched are c_{20} and g_1. As will be demonstrated later, exponential matching to u_m requires an expression for u_{01} as $x_0 \to -\infty$,

(3.32)
$$\begin{aligned}u_{01}(x_0) = &-\frac{g_1}{16}e^{-2x_0} - \frac{1}{4}c_{20}x_0 - \frac{3}{8}g_1\\ &+\frac{1}{32}\Big(2c_{20}\pi^2 + 15c_{20} + 26g_1 + (48g_1 - 12c_{20})x_0 + 24c_{20}x_0^2\Big)e^{2x_0}\\ &+\frac{1}{48}\Big(-36g_1 - 89c_{20} - 6c_{20}\pi^2 + (84c_{20} - 144g_1)x_0 - 72c_{20}x_0^2\Big)e^{4x_0} + O(e^{6x_0}),\end{aligned}$$

and then re-expanding u_0 in the variable x_m. This shows that also $c_{20} = 0$, $g_1 = 0$ and $c_{3m} = 0$. Any other choice leads to a system for the parameters having no solution. Hence, only κ_m remains as a free constant in the two regions. The exponentially matched solution is therefore simply

$$u_{01}^{(e)}(x_0) = 0\,. \tag{3.33}$$

3.1.3. $\mathbf{O(\delta^{2/3})}$.

Internal layer near κ_m. The problem of order $\delta^{2/3}$ is

$$\mathcal{L}(u_{m2}, x_m) = f_{m2}(x_m)\,, \tag{3.34a}$$

$$u_{m2}(0) = -u'_{m0}(0)\,\kappa_{m2} - \frac{1}{2}u''_{m0}\kappa_{m1}^2 - u'_{m1}(0)\kappa_{m1} = \kappa_{m2} - u'_{m1}(0)\,\kappa_{m1}\,, \tag{3.34b}$$

where

$$f_{m2}(x_m) := d_{1m}x_m^2 + d_{2m}x_m + d_{3m} + 6\,u_{m0}\,(u_{m1}^{(e)})^2\,. \tag{3.35}$$

Note that $u_{m1}^{(m)'}(0) = 0$. Again we choose the inhomogeneous solution so that it grows only algebraically as $x_m \to -\infty$ and vanishes at $x_m = 0$ to obtain (3.21) with $\alpha = m, j = 2$, and

$$\gamma_{m2} = -\frac{\pi^2}{12}d_{1m} + \ln(2)\,d_{2m} - d_{3m} - \kappa_{m1}^2\,, \tag{3.36}$$

so that the general solution is represented as

$$u_{m2}(x_m) = -\kappa_{m2}\phi_m(x_m) + \varphi_{m2}(x_m)\,. \tag{3.37}$$

As $x_m \to -\infty$, we have to compare

$$u_{m2}(x_m) = -\frac{1}{8}(d_{1m} + 2d_{3m}) - \frac{1}{4}d_{2m}x_m - \frac{1}{4}d_{1m}x_m^2 + e^{2x_m}\left(\frac{1}{64}[(-7 - 72\zeta(3))d_{1m} - 8d_{3m} + 256(\kappa_{m2} - \kappa_{m1}^2) + (30 + 4\pi^2)d_{2m}] + \frac{3}{16}(5d_{1m} - 2d_{2m} + 8d_{3m})x_m + \frac{3}{8}(2d_{2m} - d_{1m})x_m^2 + \frac{1}{2}d_{1m}x_m^3\right) + O(e^{4x_m})$$

with the outer solution. Matching the constant and the linear terms in x_m yields

$$-\frac{1}{4}d_{3m} = \frac{1}{2}A_1 - \frac{1}{8}A_1^2 + \frac{1}{3}C_1A_1 + \frac{23}{14}C_1^2 + D_1\,, \tag{3.38}$$

$$-\frac{1}{4}d_{2m} = 2^{1/6}C_1\,. \tag{3.39}$$

There is no quadratic term in the outer solution (A.10); hence $d_{1m} = 0$. There are further matching conditions, but they do not simplify the problem structurally at this point and will be enforced later, so that d_{2m}, d_{3m}, and κ_{m2} remain to be determined via exponential matching. As $x_m \to \infty$, the expansion to this order can be written as

(3.40)

$$u_{m2}^{(m)} = \frac{1}{2}d_{3m} - \frac{1}{4}d_{2m}x_m + \frac{1}{8}d_{3m}e^{2x_m} + \frac{e^{-2x_m}}{32}\Big(-56d_{3m} - 15d_{2m} - 2d_{2m}\pi^2 + 128(\kappa_{m1}^2 + \kappa_{m2}) + (48d_{3m} - 12d_{2m})x_m - 24d_{2m}x_m^2\Big) + O(e^{-4x_m})\,.$$

Internal layer near $x = 0$. As for the $O(\delta^{1/3})$ problem, at $O(\delta^{2/3})$ we have

$$\mathcal{L}(u_{02}, x_0) = f_{02}(x_0)\,, \tag{3.41a}$$

$$u_{02}(0) = 0, \quad u_{02}''(0) = 0, \quad \text{and} \quad u_{02}''''(0) = 0\,, \tag{3.41b}$$

with

$$f_{02}(x_0) := d_{10}x_0^2 + d_{20}x_0 + d_{30}\,. \tag{3.42}$$

The general solution is

$$u_{02}(x_0) = \varphi_{02}(x_0) + g_2\,\psi_0(x_0)\,, \tag{3.43}$$

where the homogeneous component is as before and the inhomogeneous part is obtained by setting $\alpha = 0$, $j = 2$, and $\gamma_{02} = 0$ in (3.21), so that $\varphi_{02}(0) = 0$ and φ_{02} grows algebraically as $x_0 \to -\infty$. Symmetry requires $\varphi_{02}''(0) = 0$, $\varphi_{02}''''(0) = 0$, which implies $d_{10} = 0$ and $d_{30} = 0$. The remaining free parameters to be matched are d_{20} and g_2. In order to exponentially match to u_m to $O(\delta^{2/3})$ and obtain $u_{m2}^{(e)}$, we again have to expand $u_{02}(x_0)$ as $x_0 \to -\infty$, giving

(3.44)

$$u_{02}(x_0) = -\frac{\hat{\mu}}{16}e^{-2x_0} - \frac{1}{4}d_{20}x_0 - \frac{3}{8}\hat{\mu} + \frac{1}{32}\Big((15 + 2\pi^2 + 2\ln(2))d_{20} + 26g_2 + (48\hat{\mu} - 12d_{20})x_0 + 24d_{20}x_0^2\Big)e^{2x_0} + \frac{1}{48}\Big(-(89 + 6\pi^2)d_{20} - 36\hat{\mu} + (84d_{20} - 144\hat{\mu})x_0 - 72d_{20}x_0^2\Big)e^{4x_0} + O(e^{6x_0})\,,$$

and re-express in terms of x_m, where we have used the abbreviation $\hat{\mu} = d_{20}\ln(2) + g_2$.

3.1.4. O(δ).

Internal layer near κ_m. The problem to be solved at order $O(\delta)$ is

$$\mathcal{L}(u_{m3}, x_m) = f_{m3}(x_m)\,, \tag{3.45a}$$

$$\begin{aligned} u_{m3}(0) = &-u'_{m2}(0)\kappa_{m1} - u''_{m0}(0)\kappa_{m1}\kappa_{m2} - u'_{m0}(0)\kappa_{m3} \\ &- \frac{1}{6}u'''_{m0}(0)\kappa_{m1}^3 - u'_{m1}(0)\kappa_{m2} - \frac{1}{2}u''_{m1}(0)\kappa_{m2}^2\,, \end{aligned} \tag{3.45b}$$

with

$$\begin{aligned} f_{m3}(x_m) := &\, 2\left((u_{m1}^{(e)})^3 + 6\,u_{m0}\,u_{m1}^{(e)}\,u_{m2}^{(e)}\right) \\ &-2^{3/2}\left[\frac{1}{2}\mathrm{dilog}(e^{2x_m}+1) + \frac{1}{2}(1+k_{1m})x_m^2 + (\ln(2)+k_{2m})x_m + k_{3m}\right]. \end{aligned} \tag{3.46}$$

Again we choose the inhomogeneous solution so that it grows only algebraically as $x_m \to -\infty$ and vanishes at $x_m = 0$ and so that we obtain $\varphi_{m3}(x_m)$ by using formula (3.21) with $\alpha = m$, $j = 3$, and $\gamma_{m3} = 0$. The solution is

$$u_{m3}(x_m) = -u_{m3}(0)\phi_m(x_m) + \varphi_{m3}(x_m)\,, \tag{3.47}$$

where k_{1m}, k_{2m}, k_{3m}, and κ_{m3} remain to be determined via matching. In order to exclude exponential growth as $x_m \to -\infty$ we obtain the relation

$$\begin{aligned} k_{2m} = \frac{\sqrt{2}}{48\ln(2)}\Big(&\kappa_{m1}\left(-(12+9\pi^2)d_{2m} + 12d_{3m} - 24\kappa_{m2}\right). \\ &+\sqrt{2}(24k_{3m} - 12\ln(2)^2 + k_{1m}\pi^2)\Big)\,, \end{aligned} \tag{3.48}$$

so that the expansion obtained as $x_m \to -\infty$ is

$$\begin{aligned} u_{m3}(x_m) = &\frac{1}{4\sqrt{2}}(1+k_{1m}+4k_{3m}) + \frac{1}{\sqrt{2}}(\ln(2)+k_{2m})x_m \\ &+ (k_{1m}+1)\frac{\sqrt{2}}{4}x_m^2 + O(e^{2x_m})\,. \end{aligned} \tag{3.49}$$

Comparing this with the outer solution to $O(\delta)$, equation (A.10), yields the matching conditions

$$\begin{aligned} \frac{1}{4\sqrt{2}}(1+k_{1m}+4k_{3m}) = &\left(-\frac{1}{4}A_1 + \frac{1}{3}C_1\right)A_2 + \left(\frac{7}{12}C_1^2 + \frac{1}{3}D_1\right)A_1 \\ &+\frac{1}{2}A_3 - \frac{59}{216}C_1A_1^2 - \frac{1}{12}2^{1/3}C_1 + K_1 - \frac{23}{7}C_1D_1 + \frac{1}{16}A_1^3 + \frac{127}{28}C_1^3 \end{aligned} \tag{3.50}$$

for the constant terms,

$$\frac{1}{\sqrt{2}}(\ln(2)+k_{2m}) = \left(D_1 - \frac{23}{7}C_1^2\right)2^{1/6} \quad \text{and} \quad (k_{1m}+1)\frac{\sqrt{2}}{4} = 2^{-2/3}C_1 \tag{3.51}$$

for the linear and the quadratic terms, respectively.

Expanding the solution as $x_m \to \infty$, we find

$$\begin{aligned} u_{m3}(x_m) = \frac{1}{192}\Big(\kappa_{m1}d_{2m}(9\pi^2+24) - 48\kappa_{m1}d_{3m} + 2\sqrt{2}\pi^2(1-k_{1m}) - 48\sqrt{2}k_{3m}\Big)e^{2x_m} \\ + \frac{1}{96}\left(\kappa_{m1}d_{2m}(27\pi^2+72) + \sqrt{2}(k_{1m}(12-6\pi^2) - 96k_{3m} - 12 + 2\pi^2)\right) \\ + \frac{1}{\sqrt{2}}(\ln(2)+k_{2m})x_m + (k_{1m}+1)\frac{\sqrt{2}}{4}x_m^2 + O(e^{-2x_m})\,, \end{aligned} \tag{3.52}$$

and we will exponentially match it to the solution near $x = 0$, which we construct next.

Internal layer near $x = 0$. The general solution to the $O(\delta)$ problem

$$\mathcal{L}(u_{03}, x_0) = f_{03}(x_0)\,, \tag{3.53a}$$

$$u_{03}(0) = 0, \quad u_{03}''(0) = 0, \quad \text{and} \quad u_{03}''''(0) = 0\,, \tag{3.53b}$$

with

$$f_{03}(x_0) := -2^{1/2}\left[\mathrm{dilog}(e^{2x_0}+1) - \mathrm{dilog}(2) + 2\mu_2 x_0 + (1+k_{10})x_0^2\right] \tag{3.54}$$

and the abbreviation $\mu_2 = \ln(2) + k_{20}$, reads

$$u_{03}(x_0) = \varphi_{03}(x_0) + g_3\,\psi_0(x_0)\,, \tag{3.55}$$

where we have required that $u_{03}(0) = 0$ and $u_{03}''(0) = 0$. If we also enforce $u_{03}''''(0) = 0$, then $k_{10} = 0$. Again we take an inhomogeneous solution $\varphi_{03}(x_0)$, which satisfies the above conditions, so that the general solution is obtained with

$$\mu_1 = \sqrt{2}(\ln(2)^2 + 2k_{20}\ln(2)) - g_3 \quad \text{and} \quad \omega = \int_0^1 \frac{1}{z}\ln\left(\frac{z^2+1}{2z}\right)^2 - \frac{\ln(2z)^2}{z}dz \approx 0.3094\,,$$

as

$$\begin{aligned} u_{03} = \frac{12\mu_1 - \pi^2\sqrt{2}}{192}e^{-2x_0} + \frac{1}{96}(36\mu_1 + \sqrt{2}(12-\pi^2)) + \frac{\mu_2}{\sqrt{2}}x_0 + \frac{\sqrt{2}}{4}x_0^2 \\ + \left[\frac{1}{192}\left(156\mu_1 + \sqrt{2}[(19-24k_{20})\pi^2 - 15 - 288\omega - 180\mu_2]\right)\right. \\ \left. + \frac{1}{16}\Big(-24\mu_1 + \sqrt{2}(12\mu_2 - 11)\Big)x_0 + \frac{\sqrt{2}}{8}(3-12\mu_2)x_0^2 - \frac{1}{\sqrt{2}}x_0^3\right]e^{2x_0} + O(e^{4x_0})\,. \end{aligned} \tag{3.56}$$

For exponentially matching to u_m this again has to be re-expressed in x_m and combined with the corresponding expressions for u_{00}, u_{01}, and u_{02} . This will be done in the next section.

3.2. Exponential matching. Now we have to match the rest of the solution $u_m(x_m)$ to the rest of the solution $u_0(x_0)$. This requires matching the exponential terms in addition to the algebraic terms, similarly to the procedure for the CCH equation; i.e., matching of the solution describing the internal layer near $x = \kappa_m$ to the solution near $x = 0$ requires expressing the variable x_0 in terms of x_m (or vice

versa). Recall again that $x_0 = x_m + \bar{\kappa}_m/\sqrt{2}$ and that $\bar{\kappa}_m < 0$; the e^{2x_0} terms in the u_0 expansion will produce e^{2x_m} terms with a factor $e^{\sqrt{2}\bar{\kappa}_m}$ (and analogously for e^{-2x_0} terms) and so we will find their corresponding matching partner at a different order in δ in the u_m expansion, as we have shown for the CCH equation. The somewhat subtle difference here is that additionally we need to determine the relationship between $e^{\sqrt{2}\bar{\kappa}_m}$ and δ, and we have in principle several choices, only one of which allows a consistent matching of both expansions. One can observe that the choice $e^{\sqrt{2}\bar{\kappa}_m} = \rho\,\delta^{1/3}$, where ρ is some constant, quickly leads to a contradiction. However, setting

$$e^{\sqrt{2}\bar{\kappa}_m} = \rho\,\delta^{2/3} \tag{3.57}$$

will lead to an $O(\delta^{2/3})$ shift of terms, so that, e.g.,

$$e^{2x_0} \quad \text{will shift to a term} \quad \delta^{2/3}\,e^{2x_m}\,, \tag{3.58}$$

$$e^{-2x_0} \quad \text{will end up as a term} \quad \delta^{-2/3}\,e^{-2x_m}, \tag{3.59}$$

and so forth, so that, e.g., a term e^{2x_0} in the leading order part of the u_0 expansion will have to match an e^{2x_m} term in the $O(\delta^{2/3})$ part of the u_m expansion, or an e^{-2x_0} term in the $O(\delta)$ part of the u_0 expansion will have to match an e^{-2x_m} term in the $O(\delta^{1/3})$ part of the u_m expansion. This will also produce terms that will have no partner term in the transformed expansion. Their coefficients must then be set to zero. If we now sum the expansions for $u_{01}(x_0)$, $u_{02}(x_0)$, and $u_{03}(x_0)$ and re-expand using (3.57), we obtain

(3.60)

$$\begin{aligned}
u_0(x_m) = -1 &- \frac{1}{16}\Big(d_{20}\ln(2) + g_2\Big)e^{-2x_m}\rho + \frac{1}{192}\left(12\mu_1 - \sqrt{2}\pi^2\right)e^{-2x_m}\,\rho\,\delta^{1/3} \\
&+\frac{1}{24}\Big(d_{20}(3\ln(\rho) - 9\ln(2) - 2\ln(\delta)) - 9g_2 - 6d_{20}x_m + 48e^{2x_m}/\rho\Big)\delta^{2/3} \\
&+\Bigg[\frac{1}{96}\Bigg(36\mu_1 + \sqrt{2}\Bigg[12 + (16\ln(\delta) - 24\ln(\rho))\mu_2 \\
&\qquad +6\left(\ln(\rho) - \frac{2}{3}\ln(\delta)\right)^2 - \pi^2\Bigg]\Bigg) \\
&+\frac{\sqrt{2}}{12}\left(2\ln(\delta) + 6\mu_2 - 3\ln(\rho)\right)x_m + \frac{\sqrt{2}}{4}x_m^2\Bigg]\delta\,,
\end{aligned}$$

which has to match $u_{m1}(x_m)$, $u_{m2}(x_m)$, and $u_{m3}(x_m)$ to each order, respectively. From this we obtain further conditions for the parameters in addition to those we have already found. Solving the complete system of equations then yields the solutions for the width of the hump

$$\Delta = \frac{\sqrt{2}}{6}\ln\left(\frac{\beta}{W(\beta^{1/3})^3}\right), \tag{3.61}$$

with $\beta = 2^{11}/(27\delta^2)$, where W is the Lambert W function (so $W(x)$ is the solution of $x = W\exp(W)$). The expressions for the remaining matching constants C_1, D_1, etc. are omitted. The first correction in (3.2) has the coefficient

$$A_1 = -3\,2^{1/6}\,. \tag{3.62}$$

Note that not only the transformed expansions but also the expressions for the parameters contain so-called *logarithmic switch-back* terms.

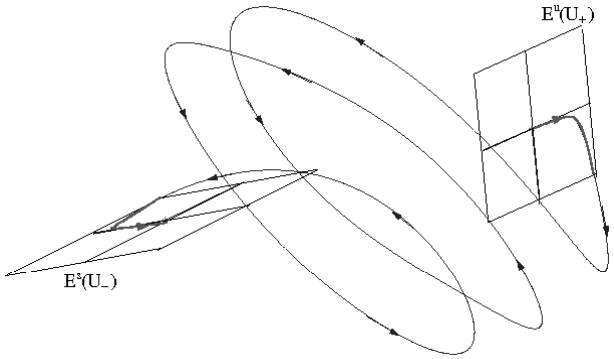

FIG. 4.1. *HCCH: Heteroclinic orbits between the equilibrium points are sought in a five-dimensional phase space that is indicated here in three dimensions. The manifolds $W^u(U^+)$ and $W^s(U^-)$ are two-dimensional, which is suggested by the two planes in the picture.*

4. Numerical method for the fifth-order phase space. For the numerical stationary solutions of the HCCH equation (3.1) we apply the same scaling for u that we used for the CCH equation to obtain equilibrium points at ± 1,

$$(1-c^2) = \frac{2}{\delta\sqrt{A}}(c_{xx} + c - Ac^3)_{xxx}\,, \quad \lim_{x\to\pm\infty} c = \mp 1, \tag{4.1}$$

again assuming that derivatives vanish in the far field. Reduction to a first-order system $U' = F(U)$, with $F : \mathrm{R}^5 \to \mathrm{R}^5$, gives a five-dimensional phase space, where the first four components of $F_i(U)$ are equal to U_{i+1} and the fifth is

$$F_5(U) = 6A(U_2)^3 + 18AU_1U_2U_3 + (3A(U_1)^2 - 1)U_4 + \delta\sqrt{A}(1-(U_1)^2)/2\,. \tag{4.2}$$

The equilibrium points are $U^\pm = \pm(1,0,0,0,0)^T$, and at these points the characteristic polynomials are

$$\mathcal{P}^\pm(\lambda) = \lambda^5 + \lambda^3(1-3A) \pm \delta\sqrt{A}\,. \tag{4.3}$$

For small δ the manifolds $W^u(U^+)$ and $W^s(U^-)$ are both two-dimensional, resulting in a codimension two event when searching for heteroclinic solutions connecting the two hyperbolic fixed points U^+ and U^-. The HCCH equation exhibits the same reversibility properties as its lower order version. This reversibility is again given by the transformation (2.8) from the CCH section, which also here fulfills $RF(U) = -F(RU)$. The codimension reduces by one and again we deal with a codimension one problem and two parameters; hence we may expect solution branches in the (A,δ) parameter plane. Section 2.1 showed that a condition for the existence of heteroclinic orbits is a value where the distance function (2.9) reaches zero, and the same condition holds for the HCCH equation. The phase space is sketched in Figure 4.1, indicating the linearizations of the intersecting manifolds in the equilibrium points. For this problem a shooting method will be very slow and may lead to inaccuracy since the additional parameter, say $\varphi \in [0, 2\pi)$, an angle defining points on a circle close to the equilibrium point on the linearization of the two-dimensional manifold, requires a very fine resolution to obtain heteroclinic solutions.

4.1. Boundary value problem formulation. There exist several possibilities for setting up equations for finding heteroclinic connections in a boundary value problem framework. Generally one crucial stumbling block is the choice of a suitable phase condition that picks out a certain solution from the infinitely many available ones due to phase shifts [8, 2]. We choose to incorporate one phase condition, proposed by Beyn [2], for which we use an approximation of the solution, V, typically given by a previous solution for slightly different parameter values. Equation (4.1) contains two parameters, A, δ, and in addition the truncated domain length L. As discussed by Doedel and Friedman [5], one of the free parameters can be replaced by L to find a connection. For a nearby chosen and fixed δ, we treat L and A as free parameters. We extrapolate in the (A, δ) plane to get an approximate value of A and solve for the exact data. Rescaling the domain to $[0, 1]$ yields, with the phase condition variable U_{ph} introduced by Beyn [2], the first-order system

$$U_i' = LU_{i+1}, \quad i = 1, 2, 3, 4, \tag{4.4a}$$

$$U_5' = L\left(6A(U_2)^3 + 18AU_1U_2U_3 + (3A(U_1)^2 - 1)U_4 + \delta\sqrt{A}\frac{(1-(U_1)^2)}{2}\right), \tag{4.4b}$$

$$U_{ph}' = L(V')^T U, \tag{4.4c}$$

$$L' = 0,\ A' = 0. \tag{4.4d}$$

Hence, we obtain one equation for the phase condition and two for the parameters in addition to the five given by the original ODE; i.e., we have an overall system of eight equations, which have to be supplemented by the same number of boundary conditions. At the edges of the domain we utilize *projected boundary conditions* [4, 2], which make use of eigenvectors in the equilibrium points and can be incorporated by computing V_0, the matrix whose columns are composed of the eigenvectors which correspond to the eigenvalues at the upper equilibrium point U^+ with negative real part, and by forming the counterpart V_1 containing those eigenvectors given by the unstable directions at the lower stationary point U^-. Hence, we consider the eight boundary conditions

$$U_{ph}(0) = 0, \quad U_{ph}(1) = 0, \quad V_0^T(U(0) - U^+) = 0, \quad V_1^T(U(1) - U^-) = 0\,. \tag{4.5}$$

For initial estimates we can use solutions obtained from the asymptotic analysis of section 3.1, i.e., the leading order solution tanh profiles

$$V(x) = -\tanh(x - K) + \tanh(x) - \tanh(x + K),$$

for the het_1 solution with guessed root-distance K.

The boundary value solvers we use are based on mono-implicit Runge–Kutta formulae [23, 14]. As for the CCH problem, efficiency can be improved by making use of the theory from section 2.1, which holds analogously for the HCCH equation, to obtain a boundary condition at the fixed point of a point-symmetric solution. We can use half of the previous domain length, and phase conditions become redundant because the phase is already fixed. We replace the projected boundary conditions by

$$U_1(0) = 1, \quad U_2(0)^2 + U_3(0)^2 = 0, \quad U_4(0)^2 + U_5(0)^2 = 0$$

so that together with the self-reversibility condition on the right interval end $U_1(1) = U_3(1) = U_5(1) = 0$ we have six conditions which match the five equations together with the free parameter A. Final solutions are obtained by reflecting the solution and its derivatives around zero and changing the signs of the first, third, and fifth components. Examples of branches of different solutions are shown in Figure 4.2.

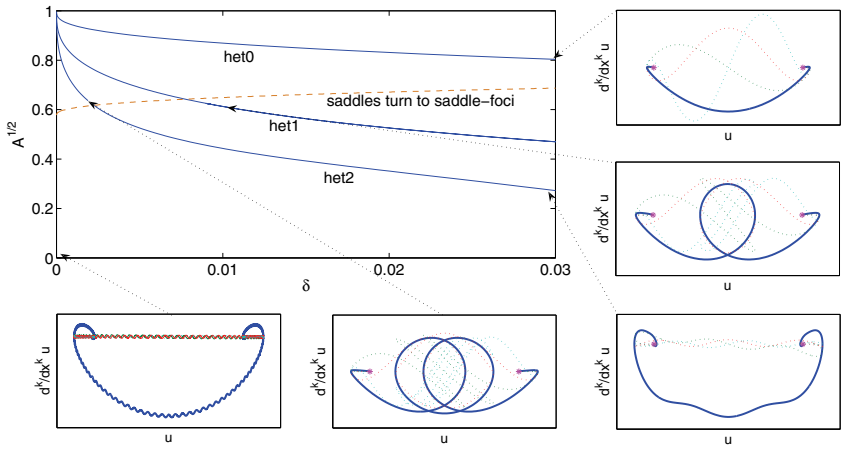

FIG. 4.2. $(\sqrt{A}, \delta)$*-plane with curves for the first three heteroclinic connection branches for the HCCH equation. The dashed line in the parameter plane indicates the position where the positive roots of the characteristic polynomial in* U^+ *have nonzero imaginary parts. Below and to the right we see five phase-space diagrams (tuples* $(U_1, U_2), (U_1, U_3), \ldots$*) for selected solutions pointed out with arrows marking the corresponding parameters. The first pair* (U_1, U_2) *is plotted as a bold solid curve.*

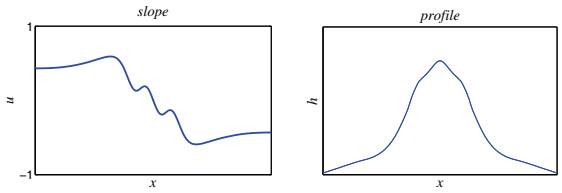

FIG. 4.3. het_2 *solution for* $\delta = 0.01$ *and* $A = 0.443$ *and the corresponding profile obtained by integration.*

4.2. Solutions and comparison to analytical results. With the boundary value formulation we are able to compute new HCCH stationary solutions. In Figure 4.3 we see a particular het_2 solution and the profile of the growing structure.

Up to three dimensions one can nicely visualize heteroclinic orbits in the corresponding phase space, while when the dimension is four or higher and the derivatives vanish in the far field one can still plot the two-dimensional phase spaces $(U_1, U_2), (U_1, U_3), \ldots$ and demand connections between the equilibrium tuples $(\pm\sqrt{A}, 0)$ as a necessary condition for heteroclinic orbits in the higher order space. Several such projections onto two dimensions are shown in Figure 4.2, where we also see a very rapidly oscillating heteroclinic curve in the bottom left plot, which was found by a shooting approach with a minimization procedure that used the two parameters and an angle as free parameters and the distance function (2.9) as an objective function, depending on those parameters. It indicates that, as shown for the CCH equation, we can in fact find many more het_k branches than those presented for $k = 0, 1, 2$, all emerging from $(A, \delta) = (1, 0)$, which corresponds to the Cahn–Hilliard equation.

In Figure 4.4 we see the change in appearance of solutions on the het_2 branch as δ is increased. The shape varies from a solution with two pronounced humps to a monotone one, similar to the het_0 solution, although associated with different,

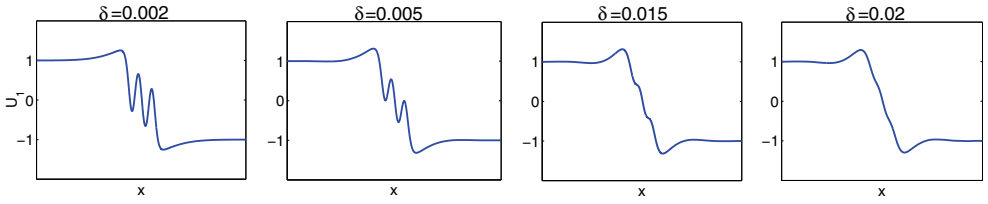

FIG. 4.4. *Structural change of the scaled het_2 solution as δ is increased.*

smaller values of A. This is crucial if one wants to compute solutions for bigger δ with a boundary value solver. It easily happens that the solver switches between solution branches; however, this can be prevented by starting continuation in a parameter regime where the high-slope parts of the solutions are nonmonotone, and continuing with small steps. A characteristic of the HCCH solutions is the overshoot from the equilibrium value before the solutions tend into the direction of the negative equilibrium point. This is not observed for the CCH equation, where the shape is similar at these regions to hyperbolic tangent functions.

In light of the expansion (3.2) we try to estimate the $\mathcal{O}(\delta^{1/3})$ terms A_1 for the different heteroclinic connections in a range of very small δ. As we see in Figure 4.5 on the left, the numerically obtained values for A behave like $A = 1 - 2^{1/6}\delta^{1/3}$ in the case of the het_0 solutions, so that $A_1 = -2^{1/6}$, which is consistent with the result in Savina et al. [22]. The numerical result for het_1 is in line with the analytical value (3.62), and since for het_2 we see the agreement $A_1 \approx -5\,2^{1/6}$, we propose for higher order trajectories that for het_k we have the general approximation $A_1 \approx -(2k+1)\,2^{1/6}$, which is reminiscent of the CCH expression (2.45). Hence this formula is used in Figure 4.5 to plot the *analytical values*.

We measure the distance between the first and second roots for the het_1 and het_2 solutions, as seen in Figure 4.5 on the right. We compare this to the analytical expression (3.61) for the 1-hump solutions in the same figure and see that for small δ the agreement is good. For both het_1 and het_2 solutions the distance is seen to increase logarithmically as δ decreases.

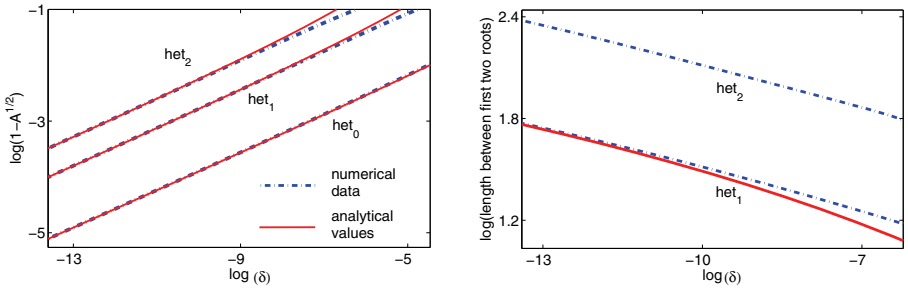

FIG. 4.5. *Left figure: Logarithmic version of the $(\sqrt{A}, \delta)$ plot for very small δ. The solid lines give the analytical values, and the dash-dotted lines give those computed with the BVP solver. On the right we see the distances between the first two roots of the het_1 and het_2 solutions numerically and for het_1 via the analytical expression* (3.61) *(solid line).*

5. Conclusion. We have demonstrated that a sixth-order generalization of the CCH equation admits multiple stationary solutions connecting constant values. As for the fourth-order CCH solution, these include a simple base solution, which is monotone for the CCH and "almost" monotone for the HCCH equation. More complex

solutions, containing multiple humps, are also possible for each value of the forcing parameter δ, given particular values of the integration constant $A(\delta)$. These non-monotone stationary solutions constitute an essential part of the solution structure for this higher order Cahn–Hilliard type of equation. We have demonstrated this via a numerical investigation of the phase space in which we are able to follow solution branches. For the simplest of the multi-humped solutions, the het_1 branch, careful use of matched asymptotics that accounts for exponentially small terms allows us to find a solution which yields both the length scale for the solution (the "hump length") and the parameter value $A(\delta)$, at which it occurs, in the limit of small δ. Extension of the analysis to higher branches appears feasible. Our numerical evidence suggests that similarly simple asymptotic expressions hold for these branches for both the CCH and HCCH equations.

Various issues, such as the stability of these solutions, are presently being considered in light of applications of the HCCH equation as a model for the morphology and dynamics of quantum dots. In particular, how do adjacent internal layers derived from these solutions interact, and what is their effect on the coarsening behavior in large spatial domains? Savina et al. [22] have begun an investigation of these questions by numerical simulation of (1.4); it is likely that asymptotics can yield further insights.

Physically, further interesting questions relate to the extension of the HCCH model to richer models for the energetics of faceted surfaces, and analyzing the three-dimensional extension of the model.

Appendix A. Outer problem. For the solution to the outer problem (3.6), (3.7) it is easy to observe that to leading order in δ the solution of

$$Q\left(Y_0\right)_{\xi\xi\xi} = -\sqrt{2}\left(Y_0^2 - 1\right) \quad \text{with} \quad \lim_{\xi\to-\infty} Y_0(\xi) = 1 \tag{A.1}$$

is

$$Y_0(\xi) = 1\,. \tag{A.2}$$

To $O(\delta^{1/3})$ the general solution to the problem

$$Y_{1_{\xi\xi\xi}} - \sqrt{2}\,Y_1 = -\frac{A_1}{\sqrt{2}} \quad \text{with} \quad \lim_{\xi\to-\infty} Y_1(\xi) = \frac{A_1}{2} \tag{A.3}$$

is

$$Y_1(\xi) = \frac{A_1}{2} + C_1 e^{2^{1/6}\xi} + e^{-\xi/2^{5/6}}\left[C_2\cos\left(\sqrt{3}\,\xi/2^{5/6}\right) + C_3\sin\left(\sqrt{3}\,\xi/2^{5/6}\right)\right], \tag{A.4}$$

with C_1, C_2, and C_3 being constants of integration. The far-field condition requires that Y_1 remains bounded as $\xi \to -\infty$. Hence, $C_2 = C_3 = 0$ and

$$Y_1(\xi) = \frac{A_1}{2} + C_1 e^{2^{1/6}\xi}. \tag{A.5}$$

Using this and the far-field conditions, the solution to the $O(\delta^{2/3})$ problem

$$Y_{2_{\xi\xi\xi}} - \sqrt{2}\,Y_2 = -\frac{A_2}{\sqrt{2}} - \frac{1}{2}\left(3\left(Y_1^2\right)_{\xi\xi\xi} - \sqrt{2}\,Y_1^2\right) \quad \text{with} \quad \lim_{\xi\to-\infty} Y_2(\xi) = \frac{A_2}{2} - \frac{A_1^2}{8} \tag{A.6}$$

is

$$Y_2(\xi) = \frac{A_2}{2} - \frac{A_1^2}{8} + D_1 e^{2^{1/6}\xi} + \frac{A_1 C_1}{3} e^{2^{1/6}\xi}\left(1 - 2^{1/6}\xi\right) - \frac{23}{14} C_1^2 e^{2^{7/6}\xi}, \tag{A.7}$$

and the solution to the $O(\delta)$ problem

$$Y_{3_{\xi\xi\xi}} - \sqrt{2}\, Y_3 = -\frac{A_2}{\sqrt{2}} + \frac{Y_{1_{\xi\xi\xi\xi}}}{4} + \sqrt{2}\, Y_1 Y_2 - \frac{1}{2}\left(Y_1^3 + 6\, Y_1 Y_2\right)_{\xi\xi\xi}$$
$$\text{with} \quad \lim_{\xi\to-\infty} Y_3(\xi) = \frac{A_3}{2} - \frac{A_1 A_2}{4} + \frac{A_1^3}{16} \tag{A.8}$$

is

$$\begin{aligned} Y_3(\xi) = {} & \frac{A_3}{2} - \frac{A_1 A_2}{4} + \frac{A_1^3}{16} \\ & + \left[K_1 - \frac{2^{1/3}}{12} C_1 + \frac{1}{3}\left(A_1 D_1 + A_2 C_1\right) - \frac{59}{216} C_1 A_1^2 \right. \\ & \left. + \left(\frac{\sqrt{2}}{12} C_1 - \frac{2^{1/6}}{3}\left(A_1 D_1 + A_2 C_1\right) + \frac{17}{72} 2^{1/6} A_1^2 C_1\right)\xi + \frac{2^{1/3}}{18} A_1^2 C_1\, \xi^2\right] e^{2^{1/6}\xi} \\ & + \left[-\frac{23}{7} C_1 D_1 + \left(\frac{7}{12} + \frac{23}{21} 2^{1/6}\xi\right) A_1 C_1^2\right] e^{2^{7/6}\xi} + \frac{127}{28} C_1^3 e^{2^{1/6} 3\xi}, \end{aligned} \tag{A.9}$$

with another integration constant K_1. Finally, we obtain the asymptotic representation in terms of x_m:

$$\begin{aligned} Y(x_m) = {} & 1 + \left[C_1 + \frac{1}{2} A_1\right] \delta^{1/3} \\ & + \left[C_1\, 2^{1/6}\, x_m - \frac{1}{8}\, A_1^2 + \frac{1}{3}\, C_1\, A_1 + D_1 - \frac{23}{14} C_1^2 + \frac{1}{2}\, A_2\right] \delta^{2/3} \\ & + \left[-\frac{23}{7} C_1^2\, 2^{1/6} x_m + D_1\, 2^{1/6} x_m + \frac{1}{2}\, C_1\, 2^{1/3} x_m^2 + \left(-\frac{1}{4}\, A_1 + \frac{1}{3}\, C_1\right) A_2 \right. \\ & \quad + \left(\frac{7}{12} C_1^2 + \frac{1}{3}\, D_1\right) A_1 + \frac{1}{2}\, A_3 - \frac{59}{216} C_1\, A_1^2 - \frac{1}{12}\, 2^{1/3}\, C_1 \\ & \quad \left. + K_1 - \frac{23}{7} C_1\, D_1 + \frac{1}{16} A_1^3 + \frac{127}{28} C_1^3\right] \delta. \end{aligned} \tag{A.10}$$

REFERENCES

[1] K. L. Adams, J. R. King, and R. H. Tew, *Beyond-all-orders effects in multiple-scales asymptotics: Travelling-wave solutions to the Kuramoto–Sivashinsky equation*, J. Engr. Math., 45 (2003), pp. 197–226.

[2] W.-J. Beyn, *The numerical computation of connecting orbits in dynamical systems*, IMA J. Numer. Anal., 9 (1990), pp. 379–405.

[3] G. Carrier and C. Pearson, *Ordinary Differential Equations*, Blaisdell, Waltham, MA, 1968.

[4] F. R. de Hoog and R. Weiss, *An approximation theory for boundary value problems on infinite intervals*, Computing, 24 (1980), pp. 227–239.
[5] E. J. Doedel and M. J. Friedman, *Numerical computation of heteroclinic orbits*, J. Comput. Appl. Math., 26 (1989), pp. 155–170.
[6] A. Eden and V. K. Kalantarov, *The convective Cahn–Hilliard equation*, Appl. Math. Lett., 20 (2007), pp. 455–461.
[7] C. L. Emmott and A. J. Bray, *Coarsening dynamics of a one-dimensional driven Cahn–Hilliard system*, Phys. Rev. E, 54 (1996), pp. 4568–4575.
[8] M. J. Friedman and E. J. Doedel, *Numerical computation and continuation of invariant manifolds connecting fixed points*, SIAM J. Numer. Anal., 28 (1991), pp. 789–808.
[9] A. A. Golovin, S. H. Davis, and A. A. Nepomnyashchy, *A convective Cahn-Hilliard model for the formation of facets and corners in crystal growth*, Phys. D, 122 (1998), pp. 202–230.
[10] A. A. Golovin, A. A. Nepomnyashchy, S. H. Davis, and M. A. Zaks, *Convective Cahn-Hilliard models: From coarsening to roughening*, Phys. Rev. Lett., 86 (2001), pp. 1550–1553.
[11] M. E. Gurtin, *Thermomechanics of Evolving Phase Boundaries in the Plane*, Clarendon Press, Oxford, UK, 1993.
[12] C. J. Howls, T. Kawai, and Y. Takei, eds., *Toward the Exact WKB Analysis of Differential Equations, Linear or Nonlinear*, Kyoto University Press, Kyoto, 1999.
[13] W. Kath, C. Knessl, and B. Matkowsky, *A variational approach to nonlinear singularly perturbed boundary value problems*, Stud. Appl. Math., 77 (1987), pp. 61–88.
[14] J. Kierzenka and L. Shampine, *A BVP solver based on residual control and the MATLAB PSE*, ACM Trans. Math. Software, 27 (2001), pp. 299–316.
[15] C. G. Lange, *On spurious solutions of singular perturbation problems*, Stud. Appl. Math., 68 (1983), pp. 227–257.
[16] K.-T. Leung, *Theory on morphological instability in driven systems*, J. Statist. Phys., 61 (1990), pp. 345–364.
[17] F. Liu and H. Metiu, *Dynamics of phase separation of crystal surfaces*, Phys. Rev. B, 48 (1993), pp. 5808–5817.
[18] R. E. O'Malley, Jr., *Phase-plane solutions to some singular perturbation problems*, J. Math. Anal. Appl., 54 (1976), pp. 449–466.
[19] L. G. Reyna and M. J. Ward, *Metastable internal layer dynamics for the viscous Cahn-Hilliard equation*, Methods Appl. Anal., 2 (1995), pp. 285–306.
[20] S. Rosenblat and R. Szeto, *Multiple solutions of nonlinear boundary-value problems*, Stud. Appl. Math., 63 (1980), pp. 99–117.
[21] Y. Saito and M. Uwaha, *Anisotropy effect on step morphology described by Kuramoto-Sivashinsky equation*, J. Phys. Soc. Japan, 65 (1996), pp. 3576–3581.
[22] T. V. Savina, A. A. Golovin, S. H. Davis, A. A. Nepomnyashchy, and P. W. Voorhees, *Faceting of a growing crystal surface by surface diffusion*, Phys. Rev. E, 67 (2003), 021606.
[23] L. F. Shampine, P. H. Muir, and H. Xu, *A user-friendly Fortran BVP-solver*, JNAIAM J. Numer. Anal. Ind. Appl. Math., 1 (2006), pp. 201–217.
[24] V. A. Shchukin and D. Bimberg, *Spontaneous ordering of nanostructures on crystal surfaces*, Rev. Modern Phys., 71 (1999), pp. 1125–1171.
[25] M. J. Ward, *Eliminating indeterminacy in singularly perturbed boundary value problems with transition invariant potentials*, Stud. Appl. Math., 87 (1992), pp. 95–134.
[26] S. J. Watson, F. Otto, B. Rubinstein, and S. H. Davis, *Coarsening dynamics of the convective Cahn-Hilliard equation*, Phys. D, 178 (2003), pp. 127–148.
[27] C. Yeung, T. Rogers, A. Hernandes-Machado, and D. Jasnow, *Phase separation dynamics in driven diffusive systems*, J. Statist. Phys., 66 (1992), pp. 1071–1088.
[28] M. A. Zaks, A. Podolny, A. A. Nepomnyashchy, and A. A. Golovin, *Periodic stationary patterns governed by a convective Cahn–Hilliard equation*, SIAM J. Appl. Math., 66 (2006), pp. 700–720.